

Effective-mass approximation in semiconductor heterostructures: One-dimensional analysis

Witold Trzeciakowski*

Division of Physics, National Research Council, Ottawa, Canada K1A 0R6

(Received 16 June 1988)

The effective-mass method (EMM) has been widely used for the description of layered semiconductor structures with sharp boundaries (quantum wells, superlattices, etc.), although it does not work for rapidly varying potentials. Here, I analyze the EMM in a simple case of one-dimensional heterostructures. Being able to obtain the exact solutions (using the transfer-matrix method), I can extract from them the envelope functions within the one-band or multiband EMM. I can then derive the boundary conditions (BC's) for these envelopes at the interfaces. These BC's turn out to be very different from what has been adopted so far. They involve microscopic parameters of the bulk materials forming the layered structures; these parameters cannot be expressed by the effective masses or other band-structure characteristics. In the multiband case the BC's are energy dependent. For the band edges of different types on two sides of the interface (as in GaAs/AlAs or Si/Ge), the BC's are unusual and allow for the existence of intrinsic interface states. I also point out some artifacts of the EMM; unphysical solutions in the bands and in the gaps which should be rejected.

I. INTRODUCTION

Since the early days of layered semiconductor structures (quantum wells, superlattices, heterojunctions) the most common approach for determining the electronic eigenstates in these materials has been the effective-mass method (EMM), sometimes also called the envelope function approximation.¹ The method has some advantages as compared to tight-binding or pseudopotential calculations. It allows the determination of the electronic states of a layered structure using only the bulk parameters of its constituents plus the value of band offsets. It can be applied self-consistently to account for charge redistribution across the interfaces, and it can also describe the effects of slowly varying perturbations on the layered structure (impurity states, magnetic- or electric-field effects, etc.). However, as it is well known, the EMM does not work for potentials rapidly varying in a unit cell, such as those introduced by the abrupt interface between two semiconductors. The correct approach, therefore, consists in applying the EMM in each layer separately and then in connecting the envelopes with appropriate boundary conditions (BC). These BC cannot be obtained from the EMM but have to be derived from microscopic considerations. This has been shown for semiconductor-insulator interfaces by Volkov and Pinsker² and by Sham and Nakayama.³ Also the effective-mass Hamiltonians which successfully describe the electronic states in bulk semiconductors, may produce some artifacts in layered materials. Therefore it is desirable to consider a simplified system where the exact solutions are available and where the EMM could be tested and boundary conditions derived. Here I have chosen to consider one-dimensional (1D) structures, periodic up to the interface (Fig. 1). Obviously this is quite idealized; interfaces may perturb at least a few atomic layers. There are also im-

portant differences between the 1D and the 3D case; I shall discuss them later. Still, I believe that this simplified model reveals some properties of real interfaces and clearly shows the artifacts of some methods applied to the 3D case. The idea of studying one-dimensional interfaces and deriving the BC for the envelopes is not new; there have been several important contributions to that problem.⁴⁻⁷ However, in all previous papers the tight-binding approximation was used. There are two important drawbacks to this approach. First, the model yields only one or two bands and, therefore, is incapable of describing the effective-mass Hamiltonians, where the terms arising from the $\mathbf{k}\cdot\mathbf{p}$ interactions with higher bands are important. Secondly, it contains several (unnecessary) assumptions so that the Hamiltonian depends on a few matrix elements that enter both the energies and the wave functions. Therefore, the relations obtained from

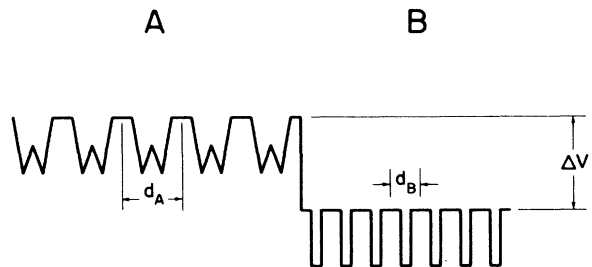


FIG. 1. The potential close to the idealized interface between 1D crystals *A* and *B*. Lattice constants are d_A and d_B . The potential discontinuity ΔV could be zero and should not be confused with the band offset W_0 . Here I chose the potentials in the unit cells to represent my initials but they are arbitrary symmetric functions.

the model might not hold in the general case. Here I present the calculation based on the transfer-matrix method which is absolutely general and yields the exact solutions for 1D crystals (or heterostructures). The number of bands is not limited and effective-mass Hamiltonians can be derived. Envelope functions can be obtained from the exact solutions and, for a heterostructure, BC for the envelopes can be determined. I have already published some preliminary results (for the one-band case).⁸

In the following I shall first briefly discuss the commonly adopted version of the EMM in the one-band and in the multiband case. I will point out some inconsistencies of the commonly adopted description which have actually led me to the present considerations (Sec. II). In Sec. III, I shall describe the transfer-matrix method which in my view is the most powerful description of a 1D crystal and could be useful for other considerations (some mathematical details can be found in the Appendixes). In Sec. IV, I discuss the one-band EMM and the BC for the envelopes. In some cases these BC allow for the existence of intrinsic interface states. In Sec. V, I discuss the multiband EMM (using mainly the two-band example, but this could be easily generalized). Section VI contains some conclusions and speculations concerning the 3D case.

II. EMM IN HETEROSTRUCTURES: THE APPROACH USED SO FAR

Let us consider the interface between two semiconductors A and B . If the band offset is small compared to the gaps in both materials and we are interested in electronic states close to the band edges, we can use the one-band EMM both in A and in B . In the direction parallel to the interface we still have translational symmetry and from the Bloch theorem the envelopes in A and B can be written as $\exp(ik_x x + ik_y y)\phi(z)$. If the band edges in A and in B are of the same type (like in GaAs/Ga_{1-x}Al_xAs with $x < 0.45$) it is usually assumed that the Bloch functions at $\mathbf{k}=\mathbf{0}$ are identical ($u_A \equiv u_B$) and that the envelopes are continuous [$\phi_A(z_0) = \phi_B(z_0)$]. As the averaged probability current along z (see Ref. 1)

$$\langle j_z \rangle \simeq \frac{-i\hbar}{2m_{\text{eff}}} \left[\frac{d\phi}{dz} \phi^* - \phi \frac{d\phi^*}{dz} \right] \quad (1)$$

should be conserved, the condition for the derivatives is

$$\frac{1}{m_A} \frac{d\phi_A(z_0)}{dz} = \frac{1}{m_B} \frac{d\phi_B(z_0)}{dz} \quad (2)$$

as first pointed out by Bastard.⁹ Here m_A and m_B are the values of the effective mass m_{eff} in A and B , respectively. These BC are sometimes “derived” by integrating across the interface) the effective-mass equation with the symmetrized kinetic-energy part (see Ref. 10 for a detailed discussion). The symmetrization is not unique, thus also the BC could take different forms. Moreover, as I emphasized in the Introduction, there is no justification for any form of the effective-mass equation for a heterostructure (i.e., across the abrupt interface).

The boundary condition of Eq. (2) allows for the ex-

istence of exponentially decaying interface states in the case when $m_A m_B < 0$, i.e., when the conduction band in A is close to the valence band in B (but there is still a gap between them). Both band edges have to be of the same symmetry. This situation can be found at the HgTe/CdTe interface.¹¹

Within the one-band EMM we replace k_z by $-i\partial/\partial z$ in the Hamiltonian. In addition to oscillatory solutions for real k_z we get exponential (evanescent) solutions for imaginary k_z ; in the bulk they would have to be rejected due to normalization condition. For a fixed (k_x, k_y) and the energy E there are always two solutions for k_z and $-k_z$ (k_z real or imaginary).

The above method is applicable only to band edges of the same type in A and B . When the minima are of different symmetry or are located in different points of the Brillouin zone, the BC have not been determined in the general case.¹² Instead, many authors investigating, e.g., GaAs/AlAs heterostructures consider the Γ and the X states separately and treat their “mixing” as a perturbation.¹³ I will show in Sec. IV that the Γ - X mixing for some energies may be important and that the perturbational approach is inadequate. The same problem arises at the Si/Ge interfaces. Also in GaSb/InAs heterostructures we have two overlapping bands of different symmetry (Γ_6 in InAs and Γ_8 in GaSb). There is more and more experimental data for heterostructures involving different types of band edges.^{13,14} I shall derive and discuss the BC for this case in Sec. IV.

Let us now discuss the multiband case. The multiband description has to be used for the valence bands, for narrow-gap materials and also when the band offsets are comparable to the gap width (like in GaSb/InAs). The prescriptions for applying the multiband EMM to layered semiconductors were discussed in several papers but in the most general form they were given by Alteralli.^{15,1} Again, the BC were either obtained by integrating the symmetrized effective-mass equation across the interface¹⁵ or by tending to zero with the quadratic terms in the Hamiltonian and thus eliminating the rapidly varying evanescent states that could modify the BC.¹⁶ Both methods are dubious because both the potential and the envelopes should be slowly varying within the framework of EMM. Anyway, band-edge Bloch functions were assumed identical on both sides of the interface. The envelopes $\phi_i(z)$ were taken to be continuous across the interface

$$\phi_i^A(z_0) = \phi_i^B(z_0), \quad i = 1, \dots, N \quad (3)$$

while their derivatives should satisfy the condition

$$\sum_{m=1}^N \left[\sum_{\alpha=x,y} (D_{lm}^{z\alpha} + D_{lm}^{\alpha z}) k_\alpha - 2iD_{lm}^{zz} \frac{d}{dz} \right] \phi_m \text{ continuous} \quad (4)$$

$$l = 1, \dots, N,$$

where the matrix $D_{lm}^{\alpha\beta}$ is determined by the quadratic part of the $\mathbf{k} \cdot \mathbf{p}$ Hamiltonian

$$H_{lm}(\mathbf{k}) = E_l(0)\delta_{lm} + \sum_{\alpha=1}^3 P_{lm}^{\alpha} k_{\alpha} + \sum_{\alpha,\beta=1}^3 D_{lm}^{\alpha\beta} k_{\alpha} k_{\beta} . \quad (5)$$

Linear terms of the Hamiltonian do not affect the boundary conditions, i.e., if we neglect the quadratic terms, we are left only with the condition (3). There were a few things that worried me in the above scheme. Basically within the EMM we can take as many bands as we wish into consideration, provided we know the parameters of the “bulk” Hamiltonian (5). Quadratic terms (apart from free-electron terms) arise from the $\mathbf{k}\cdot\mathbf{p}$ interaction with “outside” bands ($l > N$). In the bulk in many cases we can neglect these quadratic terms with good accuracy while the above BC are very sensitive to them. Another problem is the increasing number of BC when we increase N . The bulk Hamiltonian has, in general, oscillating and exponential solutions at a given energy E . The oscillating ones are simply Bloch states and for fixed (k_x, k_y) and E we usually have only two or four of them. The number of exponential solutions (“evanescent waves”) for a 3D crystal is, in principle, infinite.¹⁷ In a 1D crystal there are only two exponential solutions in the gaps because the Schrödinger equation becomes an ordinary differential equation of the second order and has two independent solutions at any energy. Therefore, it is evident that the prescription described above will fail for 1D crystals because at every energy there are only two constants that determine the wave function (in each layer) and the number of BC we have to fulfill increases with the number of bands we include in our EMM description. The EMM will give us more and more solutions as we increase N , but these will be unphysical solutions corresponding to large $|\mathbf{k}|$ values (like those encountered in Refs. 18 and 19) and should be rejected. It has to be borne in mind that EMM is based on the $\mathbf{k}\cdot\mathbf{p}$ perturbation theory and is not valid for $|\mathbf{k}|$ comparable to the Brillouin-zone radius (both for real and imaginary \mathbf{k}). Another problem with the above-described approach is that the effective-mass equations in each layer constitute a set of relations between the envelopes ϕ_i , their derivatives $\partial\phi_i/\partial z$, and, possibly, their second derivatives $\partial^2\phi_i/\partial z^2$. If we estimate the second derivatives (e.g., $\partial^2\phi_i/\partial z^2 \sim -k^2\phi_i$) we get the relation between ϕ_i and $\partial\phi_n/\partial z$. Therefore the continuity conditions for ϕ_i imply some conditions on $\partial\phi_n/\partial z$. The conditions on the envelopes and their gradients are thus interdependent and I will show, in Sec. V, on a simple example that Eqs. (3) and (4) are incompatible with the effective-mass equations. One could ask then, why was the above multiband scheme applied successfully for so many years? Well, in most cases the multiband description was used only at the start and then reduced to a one-band nonparabolic equation^{9,20} or to the problem involving fewer bands where the BC could be fulfilled after some approximations.^{18,19} In the calculations of Altarelli the BC were incorporated into a variational method¹⁵ so that they were optimized, in some sense, but did not have to be fulfilled exactly. Anyway, all these problems have inclined me to consider a simplified case where I could find the exact solutions, compare them with those obtained from EMM and, finally, *derive* the BC for the envelopes.

III. ONE-DIMENSIONAL CRYSTAL: THE TRANSFER MATRIX AND THE EMM

Let me consider the Schrödinger equation with a periodic potential $V(z) = V(z + d)$:

$$\psi''(z) + \frac{2m_0}{\hbar^2} [E - V(z)]\psi(z) = 0 . \quad (6)$$

I shall assume that $V(z)$ is symmetric around the center of each unit cell. The symmetries in 3D are much richer but at least we shall have two possible kinds of band edges—those with symmetric Bloch functions and those with antisymmetric ones. In the first cell ($0 < z < d$), following Ref. 21, I introduce two independent solutions $y_1(z)$ and $y_2(z)$:

$$y_1(0) = 1, \quad y_1'(0) = 0, \quad y_2(0) = 0, \quad y_2'(0) = 1 . \quad (7)$$

It is clear the $y_1(z)$ and $y_2(z)$ are real and independent functions. I define the transfer matrix \hat{A} in the following way:

$$\begin{aligned} A_{11} &= y_1(d), & A_{12} &= y_2(d), \\ A_{21} &= y_1'(d), & A_{22} &= y_2'(d). \end{aligned} \quad (8)$$

Any solution of Eq. (6) in the cell $0 < z < d$ can be written as a combination of y_1 and y_2 ,

$$\psi(z) = a_1 y_1(z) + b_1 y_2(z), \quad (9)$$

and in the cell $nd < z < (n+1)d$,

$$\psi(z) = a_{n+1} y_1(z - nd) + b_{n+1} y_2(z - nd). \quad (10)$$

The continuity of ψ and ψ' at the cell boundaries yields

$$\begin{pmatrix} a_{n+1} \\ b_{n+1} \end{pmatrix} = \hat{A}^n \begin{pmatrix} a_1 \\ b_1 \end{pmatrix} \quad (11)$$

which explains the term “transfer matrix.” If the potential $V(z)$ is symmetric in a unit cell it can be shown²¹ that $A_{11} = A_{22}$. The Wronskian of Eq. (6) is constant so that

$$A_{11}^2 - A_{12} A_{21} = 1 . \quad (12)$$

This means that $\det \hat{A} = 1$. The transfer matrix depends on the energy E ; we can choose two of its elements, e.g., $A_{11}(E)$ and $A_{12}(E)$, as two independent functions describing our 1D crystal. They can be determined from Eq. (6) once the potential in the unit cell is specified but for many purposes some general properties of $\hat{A}(E)$ are sufficient. I will show that many important physical quantities can be expressed by $\hat{A}(E)$.

The eigenvalues of \hat{A} ,

$$\lambda_{\pm} = A_{11} \pm (A_{12}^2 - 1)^{1/2}, \quad (13)$$

are real when $|A_{11}| > 1$ (gaps) and complex when $|A_{11}| < 1$ (bands). The wave vector \mathbf{k} defined by $\lambda_{\pm} = \exp(ik_{\pm}d)$ will then be real in the bands and complex in the gaps. From (13) we obtain

$$A_{11}(E) = \cos(kd) \quad (14)$$

which yields the band structure $E(\mathbf{k})$. At the band edges

$A_{11} = +1$ for $k=0$ or $A_{11} = -1$ for $k = \pm\pi/d$ (I shall call these points Γ and X to use the 3D analogy). In both cases $A_{12}A_{21} = 0$ [see Eq. (12)] so that there are two types of band edges at some energy E_0 : those with $A_{21}(E_0) = 0$, $A_{12}(E_0) = A_{12}^0$ (type 1), and those with $A_{12}(E_0) = 0$, $A_{21}(E_0) = A_{21}^0$ (type 2). For $k=0$ the Bloch function at the type-1 (type-2) band edge is symmetric (antisymmetric). For $k = \pm\pi/d$ it is the opposite. If I also distinguish between the bands with positive curvature (effective mass $m_{\text{eff}} > 0$) and with $m_{\text{eff}} < 0$, calling them conduction (c) and valence (v), I shall have eight different band edges: $c\Gamma 1$, $c\Gamma 2$, $cX 1$, $cX 2$, $v\Gamma 1$, $v\Gamma 2$, $vX 1$, and $vX 2$. The eigenstates of \hat{A} determine the wave functions through Eq. (10); oscillatory in the bands (Bloch states) and exponential in the gaps [see Eqs. (17) and (18)]. In an infinite crystal the exponential states would have to be rejected. In a finite slab we include them, the band structure $E(k)$ can be complemented by $E(k_r - i\mu)$ in the gaps ($k_r = 0$ at Γ gaps, $k_r = \pi/d$ at X gaps)—we get the so-called complex band structure (Refs. 22, 23, and 17). In the gaps at $k=0$ we have $\lambda_{\pm} = e^{\pm\mu d}$, $k_{\pm} = \mp i\mu$, and Eq. (14) becomes

$$A_{11}(E) = \cosh(\mu d), \quad (14a)$$

while in the gaps at $k = \pm\pi/d$ we have $k_{\pm} = \pm(\pi/d) \pm i\mu$, $\lambda_{\pm} = -e^{\mp\mu d}$, and

$$A_{11}(E) = -\cosh(\mu d). \quad (14b)$$

In the latter case we have $|\lambda_+| < |\lambda_-|$ so that the exponentially increasing eigenstates correspond to λ_- .

At this point it is instructive to consider a specific example of a 1D crystal—the Krönig-Penney potential with square wells of depth W and width a . The expressions for the transfer matrix in this case are given in Appendix A. The functions $A_{11}(E)$, $A_{12}(E)$, and $A_{21}(E)$ are shown in Figs. 2(a), 2(b), and 3(a), and 3(b) and the corresponding band structures are plotted in Figs. 2(c) and 3(c). We can see in Fig. 3 that band crossings (“zero-gap” situations) can occur,²⁴ with linear $E(k)$ dependence. Clearly, in such cases the two-band EMM would have to be used. Gaps are present also for $E > 0$ but for high energies we have to recover the free-electron case (see Appendix B). All gaps are direct, either at $k=0$ or at $k = \pm\pi/d$. Bloch states at the band edges surrounding the gap are always of opposite symmetry. At the energies close to nondegenerate band edges $E(k) \cong E_0 + \hbar^2(k - k_0)^2/2m_{\text{eff}}$ and from Eq. (14) we get

$$A_{11}(E) \cong \pm \left[1 - \frac{m_{\text{eff}}}{\hbar^2} (E - E_0) \right], \quad (15)$$

+ and - corresponding to Γ and X edges, respectively. From Eq. (12) we also get

$$A_{12}(E)A_{21}(E) \cong \frac{2m_{\text{eff}}}{\hbar^2} (E - E_0) \quad (16)$$

so that one of these functions vanishes at E_0 while the other is constant close to E_0 . If, for instance, $A_{12}(E_0) = A_{12}^0$, we get

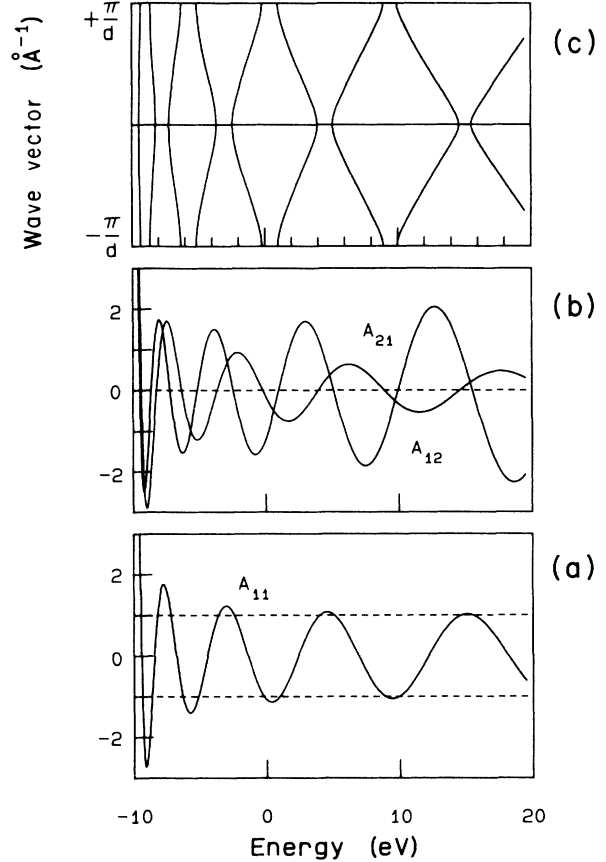


FIG. 2. (a) and (b) Elements of the transfer matrix for the Krönig-Penney case: $d = 10 \text{ \AA}$, $W = 9.75 \text{ eV}$, $a = 9.3 \text{ \AA}$. A_{11} is dimensionless, A_{12} is in \AA , A_{21} is in \AA^{-1} . (c) Corresponding real band structure.

$$A_{21}(E) \cong \frac{2m_{\text{eff}}}{\hbar^2 A_{12}^0} (E - E_0). \quad (16a)$$

Thus the transfer matrix within a one-band approximation is given by Eqs. (15) and (16); we have to know E_0 , m_{eff} , and A_{12}^0 .

Bloch functions $\psi_{\pm k}(z)$ correspond to the eigenstates of \hat{A} : $[a_{\pm}, b_{\pm}]$ with complex eigenvalues $\lambda_{\pm} = e^{\pm ikd}$. If, in the first cell our Bloch function is

$$\psi_k(z) = a_+ y_1(z) + b_+ y_2(z), \quad 0 < z < d. \quad (17)$$

Then in the $(n+1)$ th cell it becomes, according to Eq. (11),

$$\psi_k(z) = (\lambda_+)^n [a_+ y_1(z - nd) + b_+ y_2(z - nd)] = e^{ikz} u_k(z), \quad nd < z < (n+1)d \quad (18)$$

with

$$u_k(z) = e^{-ik(z - nd)} [a_+ y_1(z - nd) + b_+ y_2(z - nd)], \quad nd < z < (n+1)d. \quad (19)$$

The eigenstates $[a_{\pm}, b_{\pm}]$ should be chosen in a special way, so that the following conditions are fulfilled. (1) Bloch states $\psi_k(z)$ and $\psi_{-k}(z)$ should coincide when

$k \rightarrow 0$ or when $k \rightarrow \pi/d$ (the same must hold for exponential states in the gaps when $k = k_r - i\mu$, $k_r = 0$ or π/d). (2) Periodic Bloch amplitudes should be normalized in the standard way:

$$\frac{1}{d} \int_0^d |u_k(z)|^2 dz = 1. \quad (20)$$

Normalization of u_k is essential if we want to compare the envelopes in two different materials. From Eq. (19) we see that this requires the evaluation of the integrals $\int_0^d y_1^2$, $\int_0^d y_2^2$, and $\int_0^d y_1 y_2$. In Appendix B I show that they can be expressed by the transfer matrix and its energy derivatives. The final expressions for $[a_{\pm}, b_{\pm}]$ determining $\psi_{\pm k}$ and satisfying the above conditions are

$$[a_{\pm}, b_{\pm}] = \begin{cases} \frac{1}{\sqrt{N(E)}} [(|A_{12}|)^{1/2}, \pm \text{sgn} A_{12} (A_{21} \text{sgn} A_{12})^{1/2}] & \text{for } A_{21}(E_0) = 0 \\ \frac{1}{\sqrt{N(E)}} [\pm \text{sgn} A_{21} (A_{12} \text{sgn} A_{21})^{1/2}, (|A_{21}|)^{1/2}] & \text{for } A_{12}(E_0) = 0 \end{cases} \quad (21)$$

where $N(E)$ is the normalizing factor²⁵

$$N(E) = \begin{cases} \frac{-\hbar^2}{m_0 d} \text{sgn} A_{12} \frac{dA_{11}}{dE} & \text{for } E \text{ in the bands} \\ \frac{\hbar^2}{2m_0 d} \text{sgn} A_{12} \left[A_{21} \frac{dA_{12}}{dE} - A_{12} \frac{dA_{21}}{dE} \right] & \text{for } E \text{ in the gaps.} \end{cases} \quad (22)$$

At E close to the band edge $N(E) \approx |m_{\text{eff}}|d/m_0$, as follows from Eqs. (15) and (16). Note that the eigenstates will be real in the gaps ($A_{12}A_{21} = A_{11}^2 - 1 > 0$) and complex in the bands ($A_{12}A_{21} < 0$).

The general solution at any energy will be a combination of ψ_k and ψ_{-k} (k real in the bands, complex in the gaps). Within the one-band EMM we have¹

$$\psi_{\pm k} \cong e^{ikz} \left[u_0(z) \pm \sum_{n \neq 0} \frac{kp_{n0}}{m_0(E_n - E_0)} u_n(z) \right] \quad (23)$$

so that the general solution can be written as

$$\begin{aligned} \psi^E(z) &= \xi_1 \psi_k(z) + \xi_2 \psi_{-k}(z) \\ &\cong \phi_0(z) u_0(z) + \sum_{n \neq 0} \frac{-i\phi'_0(z)p_{n0}}{m_0(E_n - E_0)} u_n(z) \end{aligned} \quad (24)$$

with

$$\phi_0(z) = \xi_1 e^{ikz} + \xi_2 e^{-ikz} \quad (25)$$

being the envelope function.

In the multiband case we have to construct the effective-mass Hamiltonian first. In real semiconductors we can determine it from symmetry arguments and determine its parameters from experiment. In the 1D crystal we can calculate these parameters; I shall do it in the simplest case of the two-band model.

Let me consider two bands (further labeled c for the conduction band and v for the valence band) with extrema at $k=0$ and, for example, $A_{12}(E_v) = 0$, $A_{21}(E_v) = A_{21}^0$, $A_{21}(E_c) = 0$, $A_{12}(E_c) = A_{12}^0$. Therefore, the Bloch functions at the band edges will be [see Eqs. (21) and (22)]

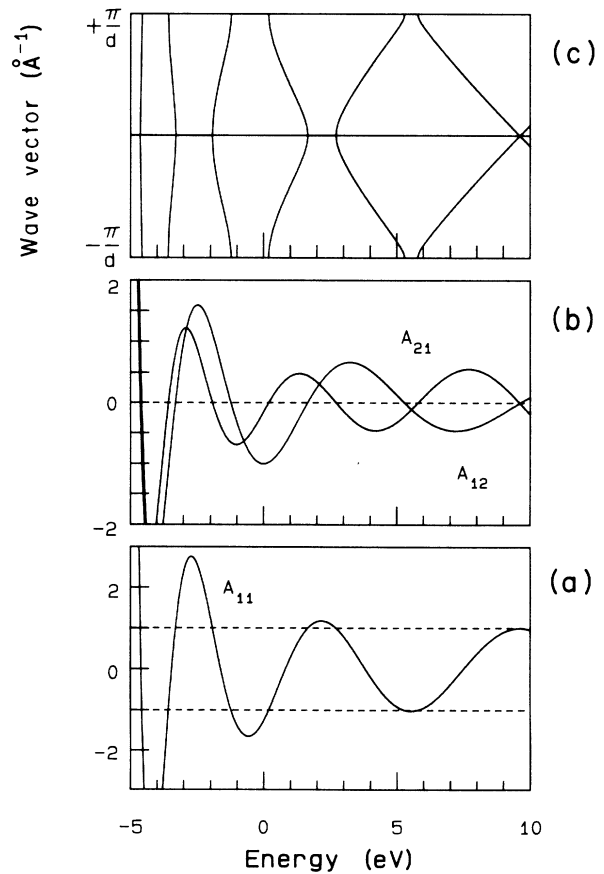


FIG. 3. Same as in Fig. 2 but for $d = 10 \text{ \AA}$, $W = 5 \text{ eV}$, $a = 8 \text{ \AA}$. Band crossing can be seen at $E \approx 9.5 \text{ eV}$. At this point $A_{11} = 1$ and both A_{12} and A_{21} vanish.

$$u_c(z) = \left[\frac{m_0}{m_c d} A_{12}^0 \right]^{1/2} y_1^{E_c}(z), \quad (26)$$

$$u_v(z) = \left[\frac{m_0}{m_v d} A_{21}^0 \right]^{1/2} y_2^{E_v}(z), \quad (27)$$

where m_c and m_v are the absolute values of the effective masses and the energy dependence of $y_1(z)$ and $y_2(z)$ is explicitly denoted.

In the Kohn-Luttinger representation the Hamiltonian ($p^2/2m_0 + V$) has the form

$$H_{nn'}^0 = \left[E_n(0) + \frac{\hbar^2 k^2}{2m_0} \right] \delta_{nn'} + \frac{\hbar}{m_0} k p_{nn'}. \quad (28)$$

In order to remove the interband terms up to second order in k we perform a transformation of our basis (see, e.g., Ref. 26) and we get

$$H_{nn'} = \left[E_n(0) + \frac{\hbar^2 k^2}{2m_0} \right] \delta_{nn'} + \frac{\hbar}{m_0} k p_{nn'} - \frac{\hbar^2 k^2}{2m_0^2} \sum_{s \neq \{n, n'\}} \left[\frac{1}{E_s - E_n} + \frac{1}{E_s - E_{n'}} \right] p_{ns} p_{sn'}. \quad (29)$$

In our simplest two-band case we have $n, n' = c, v$. The Hamiltonian becomes

$$H = \begin{bmatrix} E_v + \alpha k^2 & i\gamma_0 k \\ -i\gamma_0 k & E_c + \beta k^2 \end{bmatrix}, \quad (30)$$

where

$$\gamma_0 = \frac{i\hbar}{m_0} p_{vc} = \frac{-\hbar^2}{m_0 d} \int_0^d u_v \frac{du_c}{dz} dz, \quad (31)$$

$$\alpha = \frac{\hbar^2}{2m_0} - \frac{\hbar^2}{m_0^2} \sum_s \frac{|p_{vs}|^2}{(E_s - E_v)}, \quad (32)$$

$$\beta = \frac{\hbar^2}{2m_0} - \frac{\hbar^2}{m_0^2} \sum_s \frac{|p_{cs}|^2}{(E_s - E_c)}. \quad (33)$$

The off-diagonal quadratic terms in \hat{H} vanish, because $p_{cs} p_{sv} = 0$ due to the different symmetry of u_c and u_v . This form of $\hat{H}(k)$ was used in Refs. 1, 15, and 16 to describe the interaction between the light hole and the conduction band in GaAs/Ga_xAl_{1-x}As heterostructures. The secular equation is

$$(E_v + \alpha k^2 - E)(E_c + \beta k^2 - E) - \gamma_0^2 k^2 = 0. \quad (34)$$

This is quadratic in E so that for a given k we get two bands

$$E_c(k) = \frac{1}{2}(E_c + E_v + (\alpha + \beta)k^2 \pm \{ [E_g + (\beta - \alpha)k^2]^2 + 4\gamma_0^2 k^2 \}^{1/2}), \quad (35)$$

which for small k are parabolic:

$$E_c(k) \cong E_c + \left[\beta + \frac{\gamma_0^2}{E_g} \right] k^2, \quad (36)$$

$$E_v(k) \cong E_v + \left[\alpha - \frac{\gamma_0^2}{E_g} \right] k^2. \quad (37)$$

For any specific 1D potential the constant γ_0 can be calculated from Eq. (31) (the expression in the Krönig-Penney case is given in Appendix A) while α and β can be determined from the effective masses. The masses, in turn can be obtained from Eq. (15) once we know $A_{11}(E)$. In the real 3D crystal all these parameters would be obtained from the experiment; here we can calculate them. In the gap $k = -i\mu$ and from Eq. (35) we can get the complex band structure $E(\mu)$. If we fix the energy and look for possible values of $k^2(E)$ that satisfy Eq. (34) we get, in general, two solutions

$$k_{\pm}^2(E) = \frac{1}{2\alpha\beta} [\alpha(E - E_c) + \beta(E - E_v) + \gamma_0^2 \pm \sqrt{\Delta}] \quad (38)$$

with

$$\Delta = [\alpha(E_c - E) + \beta(E_v - E) - \gamma_0^2]^2 + 4\alpha\beta(E - E_v)(E_c - E). \quad (38a)$$

Depending on the sign of $\alpha\beta$ we have two possibilities. (1) For $\alpha\beta > 0$ we get two positive roots in the bands and one positive (real k), one negative (imaginary k) in the gap. For small values of the quadratic terms α and β one of these positive roots is very large and thus is beyond the scope of the two-band model. This was the source of the "spurious solutions" encountered in Refs. 18 and 19. (2) For $\alpha\beta < 0$ we get two negative roots in the gap (imaginary k) and one positive, one negative in the bands. This case was considered in Ref. 16 where the negative root was called the "wing band." For $\alpha > 0$, $\beta < 0$, and $\gamma_0^2/E_g < (\alpha - \beta) < 2\gamma_0^2/E_g$ we would have $\Delta < 0$ in some energy interval in the gap so that k_{\pm}^2 would be complex. In our 1D case we know the exact $k^2(E)$ which is positive in the bands and negative in the gap. Therefore, we see that the EMM can produce unphysical solutions both in the bands and in the gaps—they correspond to large $|\mathbf{k}|$ values and should be rejected. In Ref. 16 the wing bands were excluded from the wave function in the limit $\alpha, \beta \rightarrow 0$ because they become vanishingly small away from the interface. Here we can see that these wing bands should be rejected because they are the artifacts of the EMM. Any band that has a large m_{eff} (small curvature) yields large $|\mathbf{k}|$ values fairly close to the band edge. In the bulk we are seldom interested in such states but in the finite layer we often need exponential solutions lying deep in the gap with large $k = i\mu$. In three dimensions the number of exponential solutions at any energy is unlimited¹⁷ but all large- $|\mathbf{k}|$ solutions obtained from the EMM should be rejected. In one dimension it is easy to see that in our two-band model the k_+^2 solution in (38) is unphysical. It is therefore $k_-(E)$ which we compare to the exact $k(E)$ [Eqs. (14) and (A3)] in Fig. 4 for two Krönig-Penney cases. Slight discrepancies occur for higher values of k (or μ) as could be expected. The agree-

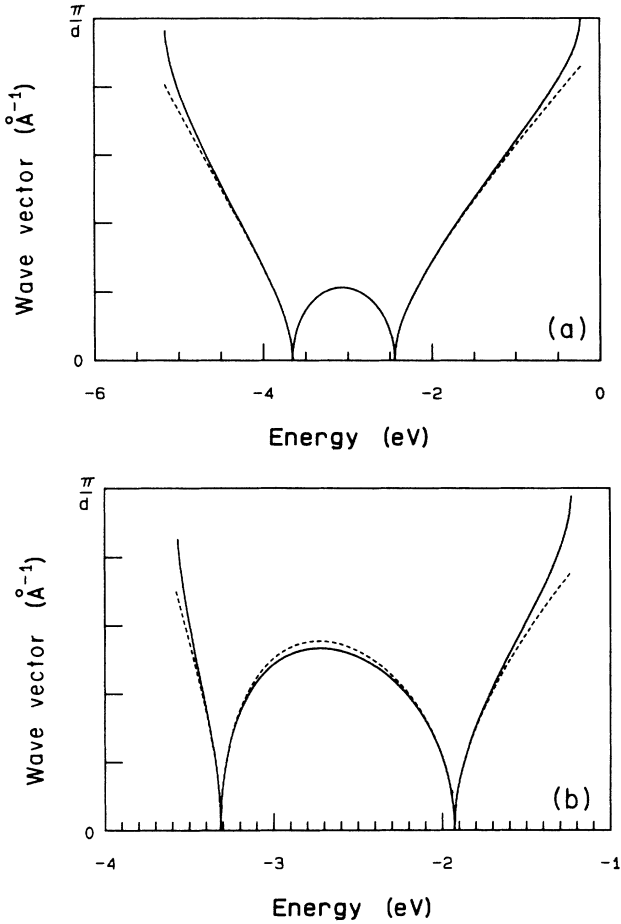


FIG. 4. Complex band structure $|k(E)|$ for the Krönig-Penney crystal in a selected energy range. Solid lines, exact; dashed lines, two-band approximation. In the bands k is real, in the gaps it is imaginary. (a) $d = 10 \text{ \AA}$, $W = 9.75 \text{ eV}$, $a = 9.3 \text{ \AA}$ [compare with Fig. 2(c)]; (b) $d = 10 \text{ \AA}$, $W = 5 \text{ eV}$, $a = 8 \text{ \AA}$ [compare with Fig. 3(c)].

ment is better when other bands are further away.

Let us now turn to the determination of the transfer matrix within the two-band approximation. This is important because I will show in the following sections that the BC are expressed by the elements of the transfer matrix. Using $k_{\pm}^2(E)$ and Eq. (14) we obtain $A_{11}(E)$ in the energy range of our two bands. $A_{12}(E)$ and $A_{21}(E)$ cannot be obtained from the band structure but, possibly, from the wave functions. Within the N -band EMM the wave function can be written as¹

$$\psi(z) \cong \sum_{l=1}^N \left[\phi_l(z) u_l(z) + \sum_{m>N} \frac{-i\phi_l' p_{lm}}{m_0[E_l(0) - E_m(0)]} u_m(z) \right]. \quad (39)$$

In an infinite crystal $\psi(z) = \psi_k(z)$, $\phi_l(z) = e^{ikz}$, and $\phi_l' = ike^{ikz}$. Very often the second term is neglected, but this is a very crude approximation. If we make it, we can

obtain expressions for $A_{12}(E)$ and $A_{21}(E)$ by inserting the exact formulas for the Bloch functions $\psi_k(z)$, $u_c(z)$, and $u_v(z)$ [Eqs. (21), (26), and (27)] and setting $z = d$. This, however, turns out to be a poor evaluation of $A(E)$ (compared, e.g., to the exact formulas in the Krönig-Penney case), especially when other bands are not far away so that the second term in Eq. (39) is important. Much better approximation for $A_{12}(E)$ and $A_{21}(E)$ can be obtained if we use the full equation (39) and the relations between the envelopes ϕ_c and ϕ_v given by the effective-mass equations. Inserting $k = -i d/dz$ into the Hamiltonian [Eq. (30)] we obtain

$$(E_v + \alpha k^2 - E)\phi_v + \gamma_0 \frac{d\phi_c}{dz} = 0, \quad (40)$$

$$-\gamma_0 \frac{d\phi_v}{dz} + (E_c + \beta k^2 - E)\phi_c = 0. \quad (41)$$

The second derivatives $\phi'' = -k^2\phi$ both for real and for imaginary k . In the bands the envelopes are combinations of e^{ikz} and e^{-ikz} , in the gaps they become combinations of $e^{\mu z}$ and $e^{-\mu z}$. This is a specific property of 1D crystals because in three dimensions we may have oscillating and exponential solutions at the same energy so that we can only estimate $\phi'' \sim -k^2\phi$. The above equations are the example of the relationships between the envelopes and the derivatives which I mentioned in Sec. II. Here we clearly see that, e.g., the boundary conditions imposed on ϕ_v imply the boundary conditions for $d\phi_c/dz$.

The envelopes can be expressed by $\hat{A}(E)$ in the following way. We can integrate Eq. (39) with $u_c(z)$ [or $u_v(z)$] in a given unit cell, thus obtaining the average value of the envelope ϕ_c^0 (or ϕ_v^0) in that cell (envelopes are slowly varying). The function $\psi(z)$ is expressed by $y_1^E(z)$ and $y_2^E(z)$ [Eq. (9)] while the band-edge Bloch functions are expressed by $y_1^{E_c}(z)$ and $y_2^{E_v}(z)$ [Eqs. (26) and (27)]. Therefore we need the values of the integrals like $\int_0^d y_1^E y_2^{E_v}$ —they are all expressed by the transfer matrix in Appendix B. We can then evaluate the envelopes in the following cell in the same way, thus obtaining ϕ_c^1 and ϕ_v^1 . This allows us to determine the approximate value of both the derivatives

$$\phi_c' \cong (\phi_c^1 - \phi_c^0)/d \quad (42)$$

and of the envelopes in between the cells

$$\phi_v \cong \frac{1}{2}(\phi_c^0 + \phi_c^1). \quad (43)$$

The relationships (40) and (41) applied to (42) and (43) yield the formulas for $A_{12}(E)$ and $A_{21}(E)$. I compared them to the exact expressions in the Krönig-Penney case and it turned out again that the accuracy was rather poor. This is due to the fact that I treated the envelopes as constant within a unit cell; also, Eqs. (42) and (43) are poor interpolations. I can go one step further, i.e., include the linear terms in $\phi_c(z)$ and $\phi_v(z)$. I obtain, in the cell $[z_0 - d/2, z_0 + d/2]$,

$$\langle \psi | u_c \rangle \cong \phi_c(z_0) + \frac{d\phi_v(z_0)}{dz} \frac{1}{d} \int u_v(z-z_0) u_c, \quad (44)$$

$$\langle \psi | u_v \rangle \cong \phi_v(z_0) + \frac{d\phi_c(z_0)}{dz} \frac{1}{d} \int u_c(z-z_0) u_v. \quad (45)$$

The integral $\int u_c z u_v$ can be easily expressed by γ_0 [Eq. (31)] and the left-hand sides of (44) and (45) can be evaluated using Eqs. (9) and (B6)–(B8) from Appendix B. The relationships (40) and (41) allow us then to determine $\phi_c(z_0)$, $\phi_v(z_0)$ and $\phi'_c(z_0)$, $\phi'_v(z_0)$. The same procedure can be repeated for the next cell, with ψ still given by Eq. (9) but

$$\begin{bmatrix} a_1 \\ b_1 \end{bmatrix} = \hat{A} \begin{bmatrix} a_0 \\ b_0 \end{bmatrix}. \quad (46)$$

$$A_{12}(E) = \left[\frac{A_{12}^0 m_v}{A_{21}^0 m_c} \right]^{1/2} \left[\frac{E - E_v}{E_c - E} \right] \frac{[1 - A_{11}(E)](k^2 d^2 - 12) \gamma_0 [1 + P_0(E - E_v - \alpha k^2)]}{6d(E - E_v - \alpha k^2) [1 + P_0(\beta k^2 + E_c - E)]}, \quad (49)$$

$$A_{21}(E) = \left[\frac{A_{21}^0 m_c}{A_{12}^0 m_v} \right]^{1/2} \left[\frac{E_c - E}{E - E_v} \right] \frac{[1 - A_{11}(E)](k^2 d^2 - 12) \gamma_0 [1 + P_0(\beta k^2 + E_c - E)]}{6d(\beta k^2 + E_c - E) [1 + P_0(E - E_v - \alpha k^2)]} \quad (50)$$

where

$$P_0 = \frac{\hbar^2}{2d\gamma_0 E_g} \left[\frac{A_{12}^0 A_{21}^0}{m_c m_v} \right]^{1/2} - \frac{1}{E_g} \quad (51)$$

and $k^2 = k_-^2(E)$ is given in Eq. (38). Therefore, in order to determine the transfer matrix from the two-band EMM we have to know additionally two “microscopic” parameters A_{12}^0 and A_{21}^0 . In the one-band case we needed only one [see Eqs. (15) and (16)]. We can plot the two-band expressions for $\hat{A}(E)$ for the Krönig-Penney crystals taking band-structure parameters together with A_{12}^0 and A_{21}^0 from the exact calculation. When compared to the exact formulas (Appendix A), the agreement is quite good (Fig. 5). Again the two-band approximation is better if other bands are further away [Fig. 5(a)].

IV. BOUNDARY CONDITIONS AND INTERFACE STATES IN THE ONE-BAND CASE

Let me now consider an idealized interface between two crystals A and B (Fig. 1). Knowing the bulk transfer matrices $\hat{A}(E)$ and $\hat{B}(E)$ I can construct the solution across the interface. Starting from a given solution $ay_1^A(z) + by_2^A(z)$ in some unit cell in A I can “propagate” it according to Eq. (11) up to the interface and then in B :

$$\begin{bmatrix} a_{N+l+1} \\ b_{N+l+1} \end{bmatrix} = \hat{B}^l \hat{A}^N \begin{bmatrix} a \\ b \end{bmatrix}. \quad (52)$$

Now the solution in the l th unit cell in B is

$$\psi(z) = a_{N+l+1} y_1^B(z - ld) + b_{N+l+1} y_2^B(z - ld). \quad (53)$$

The functions $y_1^A, y_2^A, y_1^B, y_2^B$ depend on the energy and so do the transfer matrices. If we change the potential jump at the interface ΔV (Fig. 1) we find ourselves at a different

In this way we know the envelopes $\phi_c^0, \phi_v^0, \phi_c^1$, and ϕ_v^1 , and the derivatives $\phi_c^0, \phi_v^0, \phi_c^1$, and ϕ_v^1 at two neighboring “lattice points.” Now we use a better interpolation scheme to obtain the envelopes and the derivatives in-between the lattice points:

$$\phi_c \cong \frac{1}{2}(\phi_c^0 + \phi_c^1) + \frac{d}{8}(\phi_c^{0'} - \phi_c^{1'}), \quad (47)$$

$$\phi_c' \cong \frac{3}{2d}(\phi_c^1 - \phi_c^0) - \frac{1}{4}(\phi_c^{0'} + \phi_c^{1'}), \quad (48)$$

and similarly for ϕ_v and ϕ_v' . Imposing the conditions (40) and (41) on these values we obtain the following expressions for $A_{12}(E)$ and $A_{21}(E)$:

energy in material B —our solutions in B are then modified due to the change of the transfer matrix $\hat{B}(E)$ and of the functions y_1^B and y_2^B .

Equation (52) immediately supplies us with a simple criterion for the existence of interface states: an exponentially increasing eigenstate in A should become an exponentially decreasing eigenstate in B . Here it has to be borne in mind that in the Γ gaps we have $|\lambda_+| > |\lambda_-|$ while in the X gaps $|\lambda_+| < |\lambda_-|$. Using the general form of the eigenstates given in Eq. (21) and considering all possible kinds of band edges on two sides of the interface we reach the following conclusions. (1) When the conduction band in one material is close to the valence band in another (but there is a gap left between them) the interface states can appear when both band edges are of the same type, e.g., $c\Gamma_1$ in A and $v\Gamma_1$ in B or $c\Gamma_2$ in A and vX_2 in B . (2) When two conduction (or two valence) bands meet at the interface, localized states can occur only when the band edges in A and B are of the different type, e.g., $c\Gamma_1$ in A and cX_2 in B or $v\Gamma_1$ in A and $v\Gamma_2$ in B .

The first conclusion contains as a special case the situation at the HgTe/CdTe interface¹¹ and agrees qualitatively with the condition obtained from the BC introduced by Bastard⁹ (see Sec. II). The second conclusion suggests a possibility of interface states being formed in GaAs/AlAs or in Si/Ge heterostructures.²⁷ From the proportionality of appropriate eigenstates in A and in B [using Eq. (21)] we get the condition for the interface-state energy:

$$A_{12}(E)B_{21}(E) = A_{21}(E)B_{12}(E). \quad (54)$$

For the type-1 edges at E_A in A and at E_B in B this becomes (for $m_A m_B < 0$)

$$\frac{2m_A d_A^2}{(A_{12}^0)^2 \hbar^2} (E - E_A) = \frac{2m_B d_B^2}{(B_{12}^0)^2 \hbar^2} (E - E_B). \quad (55)$$

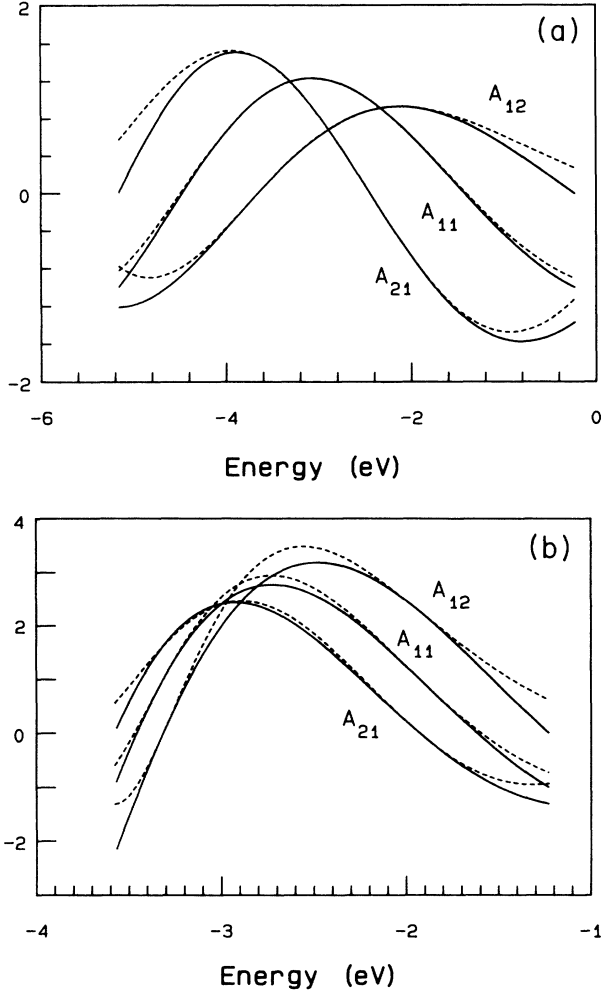


FIG. 5. The exact (solid lines) and approximate (dashed lines) elements of the transfer matrix in the Krönig-Penney case. (a) $d=10 \text{ \AA}$, $W=9.75 \text{ eV}$, $a=9.3 \text{ \AA}$; (b) $d=10 \text{ \AA}$, $W=5 \text{ eV}$, $a=8 \text{ \AA}$. Exact curves were obtained from Eqs. (A3)–(A5) while the approximate functions were calculated within the two-band model from Eqs. (14), (49), and (50) using Eq. (38) and the values of A_{12}^0 and A_{21}^0 obtained from the exact formulas. The parameters of the two-band model were also taken from the exact calculation (Appendix A).

For the type-1 edge in A and type-2 edge in B we get (for $m_A m_B > 0$)

$$\frac{2m_A d_A^2}{(A_{12}^0)^2 \hbar^2} (E - E_A) = \frac{(B_{21}^0)^2 \hbar^2}{2m_B d_B^2 (E - E_B)}. \quad (56)$$

For the type-2 edges both in A and in B the constants A_{12}^0 and B_{12}^0 in Eq. (55) should be replaced by A_{21}^0 and B_{21}^0 , respectively. The above formulas show that the energy of the intrinsic interface state can be related to A_{12}^0/B_{12}^0 or to $A_{12}^0 B_{21}^0$.

Let us now turn to the determination of the BC for the envelopes and their gradients. The exact solution is determined by Eqs. (10) and (11) in A and by Eqs. (52) and (53) in B . The normalized Bloch functions in both

materials are given in Eqs. (21) and (22). I have used two methods for obtaining the envelopes from the exact solutions: one consists in projecting the exact solution onto the band-edge Bloch functions in two neighboring cells and then interpolating in between the cells—this method will be applied in the multiband case (Sec. V) and, as I showed in Sec. III, it allows for the determination of $A_{12}(E)$ and $A_{21}(E)$. In the one-band case one can use the expressions (15) and (16) for $\hat{A}(E)$ (close to the band edges) and Eq. (25) for the envelope in A . Thus in the one-band case we can use the second method which consists in expressing the envelopes in A and B by the same constants [e.g., ξ_1 and ξ_2 from Eq. (25)] which should then cancel when determining the BC. In this approach we obtain the envelopes as continuous functions of z so that there is no need for interpolation. If we start in A from a solution $ay_1^A + by_2^A$ we can decompose

$$\begin{bmatrix} a \\ b \end{bmatrix} = \xi_1 \begin{bmatrix} a_+ \\ b_+ \end{bmatrix} + \xi_2 \begin{bmatrix} a_- \\ b_- \end{bmatrix}, \quad (57)$$

where $[a_{\pm}, b_{\pm}]$ are the eigenstates of the transfer matrix \hat{A} corresponding to eigenvalues $\lambda_{\pm} = e^{\pm ik_A d}$ (let us assume we are in the band both in material A and in material B). The envelope function in A is given by Eq. (25). In material B the wave function is given by Eqs. (52) and (53). Inserting (57) we get

$$\begin{bmatrix} a_{N+l+1} \\ b_{N+l+1} \end{bmatrix} = \hat{B}^l \left[\xi_1 \lambda_+^N \begin{bmatrix} a_+ \\ b_+ \end{bmatrix} + \xi_2 \lambda_-^N \begin{bmatrix} a_- \\ b_- \end{bmatrix} \right]. \quad (58)$$

Now if we decompose the eigenstates of \hat{A} , $[a_{\pm}, b_{\pm}]$, into the eigenstates of \hat{B} , $[\alpha_{\pm}, \beta_{\pm}]$,

$$\begin{bmatrix} a_{\pm} \\ b_{\pm} \end{bmatrix} = u_{\pm} \begin{bmatrix} \alpha_+ \\ \beta_+ \end{bmatrix} + w_{\pm} \begin{bmatrix} \alpha_- \\ \beta_- \end{bmatrix}, \quad (59)$$

we will get the required expansion similar to Eq. (24) but in B . The envelope function is

$$\begin{aligned} \phi_B(z) = & (\xi_1 e^{ik_A N d_A} u_+ + \xi_2 e^{-k_A N d_A} u_-) e^{ik_B z} \\ & + (\xi_1 e^{ik_A N d_A} w_+ + \xi_2 e^{-ik_A N d_A} w_-) e^{-ik_B z}. \end{aligned} \quad (60)$$

Here $z=0$ at the interface. Using Eq. (21) for the normalized eigenstates of \hat{A} and \hat{B} we can obtain u_{\pm}, w_{\pm} from Eq. (59) and then compare the envelopes and their gradients on both sides of the interface. This leads to the following BC:

$$\frac{\phi_B}{\phi_A} = \left| \frac{m_B}{m_A} \frac{d_B}{d_A} \frac{A_{12}^0}{B_{12}^0} \right|^{1/2}, \quad (61a)$$

$$\frac{\phi'_B}{\phi'_A} = \left| \frac{m_B}{m_A} \frac{d_A}{d_B} \frac{B_{12}^0}{A_{12}^0} \right|^{1/2} \frac{\text{sgn} m_A}{\text{sgn} m_B} \quad (61b)$$

for type-1 band edges in A and B , and

$$\frac{\phi_B}{\phi'_A} = \left| \frac{m_B}{m_A} \frac{d_A d_B}{A_{12}^0 B_{21}^0} \right|^{1/2} \text{sgn} m_A, \quad (62a)$$

$$\frac{\phi_A}{\phi'_B} = \left| \frac{m_A}{m_B} \frac{d_A d_B}{A_{12}^0 B_{21}^0} \right|^{1/2} (-\text{sgn} m_B), \quad (62b)$$

for the type-1 band edge in A and type-2 edge in B . For the type-2 edges both in A and in B the BC are determined by Eqs. (61) with the replacement $1 \leftrightarrow 2$.

It is easy to check in each case that the average probability current, proportional to $[\phi(\phi')^* - \phi'\phi^*]/m_{\text{eff}}$, is conserved across the interface. The products $\phi\phi'$ contain only the effective masses but, e.g., the logarithmic derivatives depend only on the microscopic parameters like d_A and A_{12}^0 . The masses can be removed from the above BC (except for the signs) by the transformation $\tilde{\phi} = \phi/|m_{\text{eff}}|^{1/2}$ suggested in Ref. 5. This shows that the masses will only affect the envelope functions but have no direct influence on the energies [the masses enter only through the $E(k)$ dependence in each material]. In the transfer-matrix method the effective masses and the whole band structure are determined by $A_{11}(E)$ [see Eq. (14)] while the BC contain the off-diagonal elements A_{12}^0 or A_{21}^0 , independent of A_{11} . The ratio A_{12}^0/B_{12}^0 is not related to the ratio m_B/m_A even when the Bloch functions in A and B are almost identical ($u_A \approx u_B$); this can be checked numerically for, e.g., the Krönig-Penney crystals or analytically from Eq. (6) treating $V_A - V_B$ as a perturbation. Concluding, the BC for the envelopes contain microscopic parameters of the two crystals, even for an idealized interface. These parameters are not related to the effective masses and can be determined from first-principles calculations¹² but, at the moment, they can be treated as fitting constants, similarly to band offsets. The case of abrupt heterojunctions resembles the case of deep impurities or, better, the chemical shift of shallow impurities where we need additional characteristics of the rapidly varying potential. Thus, the attempts to construct the effective-mass Hamiltonian for an abrupt heterojunction¹⁰ should be abandoned. It is also interesting to note that the Bloch functions in A and B can be quite different and still it is possible to formulate the BC for the envelopes. The previous statements concerning the interface states are confirmed here: for two bands of the same type the masses must be of the opposite signs, for the bands of different types in A and in B the masses have to be of the same sign.

Although the BC given in Eqs. (61) differ from the ones used before, the effect they have on, e.g., the energy levels of a single quantum well is rather small, especially for deep wells. When the wave function decays rapidly in the barrier, the matching conditions are not that essential. Still, they might be important for the resonant tunneling or for the superlattice band structure. The BC for two different types of band edges in A and B [Eqs. (62)] are rather unusual. They coincide with those obtained by Ando and Mori⁶ for the case $m_A > 0$ and $m_B < 0$ to describe the GaSb-InAs interface. The BC from Eq. (62) modify the bound states in a quantum well BAB in an unexpected way. Let us assume $d_A = d_B = d$, $m_A > 0$, and $m_B > 0$, in the barriers $B_{12}(E_B) = 0$ and in the well $A_{21}(E_A) = 0$. The well extends from $-L/2$ to $L/2$. Denoting $W_0 = E_B - E_A$ (depth of the well), $\alpha = |A_{12}^0 B_{21}^0|$ ("microscopic parameter"), $E - E_A = \hbar^2 k^2 / 2m_A$, and $E_B - E = \hbar^2 \mu^2 / 2m_B$ the following conditions for the bound states are obtained:

$$\tan \frac{kL}{2} = \frac{-\alpha}{d^2 \mu k} \quad (63)$$

for symmetric solutions and

$$\tan \frac{kL}{2} = \frac{\mu k d^2}{\alpha}, \quad (64)$$

for antisymmetric solutions. For the states below the bottom of the well (interface states) we may use Eqs. (63) and (64) with $k = i\xi$. The antisymmetric interface state lies above the symmetric one and with increasing well depth it crosses the bottom of the well and becomes the lowest state inside the well. A similar transition can be obtained for a fixed depth but with decreasing well width. The condition for antisymmetric state to lie below the bottom of the well is

$$W_0 < \left[\frac{\alpha L}{2d} \right]^2 \frac{\hbar^2}{2m_B d^2}. \quad (65)$$

For deep wells the spectrum is similar to the standard case: $E_n \approx \hbar^2 n^2 \pi^2 / 2m_A L^2$. However, the symmetric and antisymmetric solutions change places and we always have the symmetric interface state below the well. I expect the GaAs well with AlAs barriers to reveal some of the above-described properties (see Sec. VI).

V. BOUNDARY CONDITIONS IN THE MULTIBAND CASE

Throughout this section I shall use the two-band model (discussed already in Sec. III) as an illustration of the multiband case. Thus I assume that in both materials A and B forming the interface we can use the EMM Hamiltonians given in Eq. (30) with $k = -i d/dz$. All parameters of these Hamiltonians will now have A or B indices. I will also assume that the band edges are at the Γ point in A and in B and that both conduction-band edges are type 1 and both valence-band edges are type 2. This means that the Bloch functions will be given by Eqs. (26) and (27). I also take $d_A = d_B = d$. In each material the (real or complex) wave vector $k(E)$ is given by Eq. (38). This wave vector inserted into Eq. (14) yields the diagonal element of the transfer matrix [$A_{11}(E)$ or $B_{11}(E)$] while the off-diagonal ones ($A_{12}, B_{12}, A_{21}, B_{21}$) are determined by Eqs. (49) and (50). The exact solution is determined by the transfer matrices through Eqs. (10) and (11) (in material A) and through Eqs. (52) and (53) in material B . Now it is necessary to determine the values of the envelopes and their gradients on both sides of the interface. It is sufficient to consider only two neighboring cells to the left and to the right of the interface (denoted by 0 and 1, respectively). In the cell on the A side we have

$$\psi_0^A(z) = ay_1^A(z+d) + by_2^A(z+d) \quad (66)$$

while in the cell on the B side we have

$$\psi_1^B(z) = a'y_1^B(z) + b'y_2^B(z) \quad (67)$$

with

$$\begin{bmatrix} a' \\ b' \end{bmatrix} = \hat{A} \begin{bmatrix} a \\ b \end{bmatrix}. \quad (68)$$

If A was extending further to the right we would have

$$\psi_1^A(z) = a'y_1^A(z) + b'y_2^A(z) \quad (69)$$

in the cell to the right of the interface. Similarly, if B was extending further to the left we would have

$$\psi_0^B(z) = a''y_1^B(z+d) + b''y_2^B(z+d) \quad (70)$$

with

$$\begin{bmatrix} a'' \\ b'' \end{bmatrix} = \hat{B}^{-1} \begin{bmatrix} a' \\ b' \end{bmatrix} = \hat{B}^{-1} \hat{A} \begin{bmatrix} a \\ b \end{bmatrix}. \quad (71)$$

These fictitious extensions allow us to determine the interpolated values of the envelopes and their gradients at the interface. The method is exactly the same as the one described in Sec. III [Eqs. (44)–(48)]. Due to Eqs. (68) and (71) all envelopes and gradients contain only combinations of a and b ; these combinations cancel in boundary conditions. If we insert the expressions for $A_{12}(E)$ and $A_{21}(E)$ [Eqs. (49) and (50)] into these BC we finally obtain

$$\frac{\phi_c^A}{\phi_c^B} = f_c(E) \frac{E_c^B - E + [\beta^B - P_0^B(\gamma_0^B)^2]k_B^2}{E_c^A - E + [\beta^A - P_0^A(\gamma_0^A)^2]k_A^2}, \quad (72)$$

$$\frac{\phi_v^A}{\phi_v^B} = f_v(E) \frac{E_v^B - E + [\alpha^B + P_0^B(\gamma_0^B)^2]k_B^2}{E_v^A - E + [\alpha^A + P_0^A(\gamma_0^A)^2]k_A^2}, \quad (73)$$

$$\frac{\phi_c^{A'}}{\phi_c^{B'}} = f_v(E) \frac{\gamma_0^B + P_0^B \gamma_0^B (\beta^B k_B^2 + E_c^B - E)}{\gamma_0^A + P_0^A \gamma_0^A (\beta^A k_A^2 + E_c^A - E)}, \quad (74)$$

$$\frac{\phi_v^{A'}}{\phi_v^{B'}} = f_c(E) \frac{\gamma_0^B + P_0^B \gamma_0^B (E - E_v^B - \alpha^B k_B^2)}{\gamma_0^A + P_0^A \gamma_0^A (E - E_v^A - \alpha^A k_A^2)}, \quad (75)$$

where

$$f_c(E) = \left[\frac{A_{21}^0 m_v^B}{B_{21}^0 m_v^A} \right]^{1/2} \frac{(E - E_v^B)}{(E - E_v^A)} \times \frac{[1 - A_{11}(E)](k_A^2 d^2 + 24)\gamma_0^A}{[1 - B_{11}(E)](k_B^2 d^2 + 24)\gamma_0^B}, \quad (76)$$

$$f_v(E) = \left[\frac{A_{12}^0 m_c^B}{B_{12}^0 m_c^A} \right]^{1/2} \frac{(E - E_c^B)}{(E - E_c^A)} \times \frac{[1 - A_{11}(E)](k_A^2 d^2 + 24)\gamma_0^A}{[1 - B_{11}(E)](k_B^2 d^2 + 24)\gamma_0^B}. \quad (77)$$

Here, as usual, $k^2(E)$ is positive in the bands, negative in the gaps, and it should be determined from Eq. (38). $A_{11}(E)$ is again determined by Eqs. (14) or (14a), P_0 is given in Eq. (51). The above BC are energy dependent and in addition to band-structure parameters they contain microscopic constants A_{12}^0, A_{21}^0 and B_{12}^0, B_{21}^0 . For $E \approx E_c^A \approx E_c^B$ or for $E \approx E_v^A \approx E_v^B$ they reduce to the BC in the one-band case [Eq. (61)]. The conditions for the gradients follow from the conditions for the envelopes (and vice versa) if we use Eqs. (40) and (41) so that only two of

the above BC are independent. Formally the more bands we include in our EMM the more BC we obtain; but the important thing is that some of them are redundant. For the 2×2 Hamiltonian of Eq. (30) the BC introduced by Altarelli would read [see Eqs. (3) and (4)]

$$\frac{\phi_c^A}{\phi_c^B} = 1 = \frac{\phi_v^A}{\phi_v^B}, \quad (78)$$

$$\frac{\phi_c^{A'}}{\phi_c^{B'}} = \frac{\beta^B}{\beta^A}, \quad (79)$$

$$\frac{\phi_v^{A'}}{\phi_v^{B'}} = \frac{\alpha^B}{\alpha^A}. \quad (80)$$

These BC are independent of each other—furthermore, they are incompatible with the effective-mass equations (40) and (41). The conditions for the gradients do not reduce to the one-band condition [Eq. (2)] in the appropriate limit.²⁸

For the two-band model we can consider a specific case when the “microscopic” potentials in A and in B are identical but only shifted by a constant amount ΔV . In this case the band-edge Bloch functions will be identical in A and in B and also $A_{12}^0 = B_{12}^0, A_{21}^0 = B_{21}^0, \alpha^A = \alpha^B, \beta^A = \beta^B$, etc. In Fig. 6 I plotted the right-hand side of Eqs. (72)–(75) in the Krönig-Penney case (A_{12}^0 and A_{21}^0 were determined from the exact formulas, see Appendix A). In the energy range correctly described by the two-band model (see the band structure in Fig. 4) the envelope ratio is almost constant and of the order of unity [so that

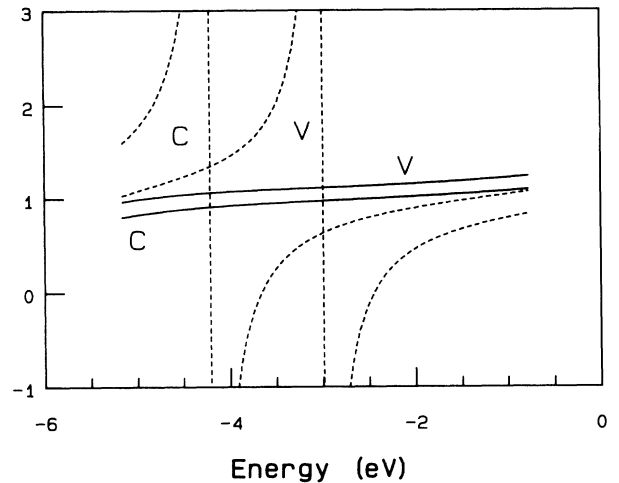


FIG. 6. Boundary conditions [Eqs. (72)–(75)] for the envelopes and their gradients at the interface between two Krönig-Penney crystals: $d = 10 \text{ \AA}$, $W = 9.75 \text{ eV}$, $a = 9.3 \text{ \AA}$ [see Figs. 2 and 4(a)], potential jump $\Delta V = 548 \text{ meV}$ (in this case ΔV is equal to the band offset). Envelope ratio at the interface, solid lines; gradient ratio, dashed lines. In both cases c and v denote the conduction- and valence-band envelopes, respectively. The BC used previously would imply [see Eqs. (78)–(80)] that all these ratios should be equal to unity.

Eq. (78) is approximately correct] but the gradient ratio strongly varies with energy. $\phi_c^{A'}/\phi_c^{B'}$ has a singularity at $E = E_v^B$, $\phi_v^{A'}/\phi_v^{B'}$ at $E = E_c^B$. This is also evident from Eqs. (40) and (41) if the envelopes are almost continuous. The conditions (79) and (80) ("old BC") are therefore totally incorrect.

VI. SUMMARY AND CONCLUSIONS

Here I would like to discuss what we can learn from the analysis of the one-dimensional case as far as the EMM in real heterostructures is concerned. Despite all the differences between the 1D case and the 3D layered structures certain conclusions are generally true. (1) The EMM is not valid for a layered material with some "superlattice potential;" it can only be applied to separate layers and then the envelopes should be properly matched at the interfaces. (2) The EMM in a finite layer can produce unphysical exponential and oscillating solutions corresponding to large $|k_z|$. These solutions should be rejected. (3) The BC used so far are incorrect, both in the one-band and in the multiband case. The proper BC involve some microscopic parameters not related to the effective masses. These parameters should either be determined from first principles or treated as fitting constants. For the most common heterostructure GaAs/Al_xGa_{1-x}As with $x < 0.4$ we can probably assume that the ratio of these parameters is close to unity (see Ref. 12) but for very different materials this cannot be postponed.

For the band edges of different symmetry in two materials the BC can be very unusual, allowing for the existence of slowly varying interface states and leading to unusual properties of a quantum well or a resonant tunneling structure formed from these materials.

At this point it is worthwhile to comment on the approach, commonly adopted for GaAs/AlAs heterostructures, namely the separate consideration of Γ and X profiles (see, e.g., Refs. 13 and 14). Within such approach there is no place for, e.g., bound states in the Γ - X well considered in Sec. IV. There is more and more experimental evidence for such states in GaAs/AlAs resonant tunneling structures.^{14,29} There is also strong evidence that there are interface states at the GaAs/AlAs interface;³⁰ they might be extrinsic but I believe that this problem requires more experimental investigation.

Another important case of band edges of different symmetry can be found in Si/Ge heterostructures. Here the band structure is strongly modified by the strain which, in turn, depends on the substrate on which the structure is grown. The conduction-band minima are located in different regions of the Brillouin zone so that the EMM is difficult to apply. The conduction-band offset seems to be very small in this case³¹ but one could search for the interface states in the gap.

The third interesting case is the GaAs/Ge heterojunction, preferably grown along the (111) direction.³² This would allow the Bloch states with small (k_x, k_y) to propagate across the interface from Γ minimum in GaAs to L minima in Ge along the growth direction.

Finally, the case which can be described within a one-

band picture (in a certain energy range) but involves two bands of different symmetry; the GaSb/InAs superlattice.³³ The simplest way to describe the superlattice (SL) is to use the transfer-matrix method—this time the SL unit cell consists of, say, one InAs layer (thickness d_1) surrounded by two layers of GaSb (thickness $d_2/2$). The SL periodicity is $d = d_1 + d_2$ and the unit cell is symmetric. Also, at the boundaries between unit cells we have the continuity of envelopes and their gradients so that the formalism described in Sec. III applies without any changes. Of course, in order to determine the transfer matrix $\hat{A}^{\text{SL}}(E)$ we have to propagate the solutions $y_1(z)$ and $y_2(z)$ across two GaSb/InAs boundaries where the BC given in Eq. (62) will hold. In the most interesting energy range of the overlapping conduction band in InAs and valence band in GaSb we obtain

$$A_{11}^{\text{SL}}(E) = -\cos(k_1 d_1) \cos(k_2 d_2) - \frac{1}{2} \sin(k_1 d_2) \sin(k_2 d_2) \times \left[\frac{k_1 k_2 d^2}{\alpha} + \frac{\alpha}{k_1 k_2 d^2} \right], \quad (81)$$

where $\hbar^2 k_1^2 / 2m_c = E - E_c$ in InAs conduction band and $\hbar^2 k_2^2 / 2m_v = E_v - E$ in the (GaSb) valence band. Here again $\alpha = |A_{12}^0 B_{21}^0|$ is the microscopic parameter characterizing the interface (see Sec. IV). The SL band structure is given by $A_{11}^{\text{SL}}(E) = \cos(kd)$. It is quite different from those obtained by Sai-Halasz and by Altarelli (Ref. 33). This is only the first step of the calculation; after determining the position of the Fermi level and after calculating the charge transfer between the GaSb and InAs layers the new potential in the layers should be determined, leading to a new $A_{11}^{\text{SL}}(E)$. Here I just want to point out that the BC have a very important effect on the final spectrum.

In the multiband case the BC are energy dependent, especially for the gradients. They also depend on each other; the correct multiband BC must be compatible with the effective-mass equations in the bulk material. For example, narrow-gap zinc-blende semiconductors are well described by the $8 \times 8 \mathbf{k} \cdot \mathbf{p}$ Hamiltonian without the quadratic terms (see, e.g., Ref. 34). This model allows us to express all envelopes by the first two: ϕ_1 and ϕ_2 . Therefore the only independent BC will be those for ϕ_1 and ϕ_2 . In this way the number of BC does not necessarily increase with the number of bands included in the EMM.

I should stress that all my statements about the real heterostructures are speculative because of obvious differences between the 1D and the 3D case. For any quantitative predictions numerical calculations for specific interfaces are required. Such calculations for GaAs/Al_xGa_{1-x}As interfaces have recently been reported¹² and the 1D model with the exact solutions can always be used to test the accuracy of more realistic (but approximate) calculations. The EMM is such a useful and important method for heterostructures that it is certainly worth further effort.

ACKNOWLEDGMENTS

I am very grateful to Dr. M. Altarelli and Dr. P. Hawrylak for fruitful discussions.

APPENDIX A: THE KRÖNIG-PENNEY CASE

Here I would like to write down the transfer matrix $\hat{A}(E)$ and other important quantities for a potential with periodicity d consisting of square wells with the width a and depth W :

$$V(z) = \begin{cases} -W & \text{for } \frac{d-a}{2} < z < \frac{d+a}{2} \\ 0 & \text{for } 0 < z < \frac{d-a}{2} \text{ and } \frac{d+a}{2} < z < d, \end{cases} \quad (\text{A1})$$

$$V(z+nd) = V(z). \quad (\text{A2})$$

Using the definition of the transfer matrix [Eq. (8)] and determining $y_1(z)$ and $y_2(z)$ satisfying Eq. (7) we obtain

$$A_{11} = A_{22} = \frac{\kappa^2 - k^2}{2\kappa k} \sin(ka) \sinh[\kappa(d-a)] + \cos(ka) \cosh[\kappa(d-a)], \quad (\text{A3})$$

$$\gamma_0 = \frac{-\hbar^2 (A_{12}^0 A_{21}^0)^{1/2}}{d^2 (m_c m_v)^{1/2} \kappa_v} \left[\frac{k_c \cosh \kappa_c \frac{d-a}{2} \sinh \kappa_v \frac{(d-a)}{2}}{\cos k_c \frac{a}{2} \sin k_v \frac{a}{2}} \left[\frac{\sin(k_c - k_v) \frac{a}{2}}{(k_c - k_v)} - \frac{\sin(k_c + k_v) \frac{a}{2}}{(k_c + k_v)} \right] + \kappa_c \left[\frac{\sinh(\kappa_v + \kappa_c) \frac{(d-a)}{2}}{(\kappa_v + \kappa_c)} + \frac{\sinh(\kappa_c - \kappa_v) \frac{(d-a)}{2}}{\kappa_v - \kappa_c} \right] \right], \quad (\text{A6})$$

where

$$\kappa_c^2 = -2m_0 E_c / \hbar^2,$$

$$\kappa_v^2 = 2m_0 (E_c + W) / \hbar^2.$$

E_c , E_v , m_c , and m_v are determined from $A_{11}(E)$ [Eqs. (15) and (A3)], while the parameters $A_{12}^0 = A_{12}(E_c)$ and $A_{21}^0 = A_{21}(E_v)$ are determined from Eqs. (A4) and (A5).

The two remaining parameters of the 2×2 Hamiltonian (α and β) are obtained from m_c and m_v [see Eqs. (36) and (37)].

APPENDIX B: SOME USEFUL FORMULAS FOR A 1D CRYSTAL

Here I would like to derive several identities involving the transfer matrix, using only the Schrödinger equation [Eq. (6)] for a periodic potential $V(z+d) = V(z)$. For very high energies ($E \gg V$) this equation becomes

$$\psi'' + \frac{2m_0}{\hbar^2} E \psi = 0 \quad (\text{B1})$$

so that its solutions are combinations of $\sin(kx)$ and

$$A_{12} = \frac{\sin(ka)}{2\kappa^2 k} \{ \kappa^2 + k^2 + (\kappa^2 - k^2) \cosh[\kappa(d-a)] \} + \frac{1}{\kappa} \cos(ka) \sinh[\kappa(d-a)], \quad (\text{A4})$$

$$A_{21} = \frac{\sin(ka)}{2k} \{ -\kappa^2 - k^2 + (\kappa^2 - k^2) \cosh[\kappa(d-a)] \} + \kappa \cos(ka) \sinh[\kappa(d-a)], \quad (\text{A5})$$

where $\kappa^2 = -2m_0 E / \hbar^2$, $k^2 = 2m_0 (E + W) / \hbar^2$. These formulas hold for $E < 0$ and for $E > 0$. For the latter case κ becomes imaginary, $(1/\kappa) \sinh[\kappa(d-a)]$ becomes $(1/|\kappa|) \sin[|\kappa|(d-a)]$, etc. The examples of $A_{11}(E)$, $A_{12}(E)$, and $A_{21}(E)$ are given in Figs. 2 and 3 together with the band structure $E(k)$ following from $A_{11}(E) = \cos(kd)$.

Using the two-band model we need the value of γ_0 —the matrix element of momentum between two band-edge Bloch functions [Eq. (31)]. Inserting Eqs. (26) and (27) into Eq. (31) we obtain

$\cos(kx)$. Determining the $y_1(z)$ and $y_2(z)$ solutions [Eq. (7)] and using the definition of the transfer matrix $\hat{A}(E)$ [Eq. (8)] we obtain

$$A_{11}(E) = A_{22}(E) = \cos \left[\frac{E}{E_0} \right]^{1/2}, \quad (\text{B2})$$

$$A_{12}(E) = d \left[\frac{E_0}{E} \right]^{1/2} \sin \left[\frac{E}{E_0} \right]^{1/2}, \quad (\text{B3})$$

$$A_{21}(E) = -\frac{1}{d} \left[\frac{E}{E_0} \right]^{1/2} \sin \left[\frac{E}{E_0} \right]^{1/2}, \quad (\text{B4})$$

where $E_0 = \hbar^2 / (2m_0 d^2)$. These are the asymptotic expressions for the transfer matrix. There are no gaps and at the band edges for $E = E_0 n^2 \pi^2$ both A_{12} and A_{21} vanish. Now let me consider the full Eq. (6) for two different energies E_c and E_v and two corresponding functions ψ_c and ψ_v . Multiplying the first ψ_v and the second by ψ_c and subtracting I get

$$\psi_c'' \psi_v - \psi_c \psi_v'' = \frac{d}{dz} (\psi_c' \psi_v - \psi_v' \psi_c) = -\frac{2m_0}{\hbar^2} (E_c - E_v) \psi_c \psi_v. \quad (\text{B5})$$

For $E_c = E_v$ we simply get the constancy of the Wronskian. For different energies Eq. (B5) leads to useful identities for the integrals of $y_1(z)$ and $y_2(z)$. Integrating (B5) from 0 to d and using the definition of the transfer matrix we obtain

$$-\frac{2m_0}{\hbar^2}(E_c - E_v) \int_0^d y_1^{E_c} y_1^{E_v} = A_{21}(E_c) A_{11}(E_v) - A_{21}(E_v) A_{11}(E_c), \quad (\text{B6})$$

$$-\frac{2m_0}{\hbar^2}(E_c - E_v) \int_0^d y_1^{E_c} y_2^{E_v} = A_{21}(E_c) A_{12}(E_v) - A_{11}(E_v) A_{11}(E_c) + 1, \quad (\text{B7})$$

$$-\frac{2m_0}{\hbar^2}(E_c - E_v) \int_0^d y_2^{E_c} y_2^{E_v} = A_{11}(E_c) A_{12}(E_v) - A_{11}(E_v) A_{12}(E_c). \quad (\text{B8})$$

Here E_c and E_v are arbitrary energies—if they correspond to the band edges, Eqs. (B6)–(B8) further simplify. If, for arbitrary E_v we tend with E_c to E_v , we can expand the functions on the right-hand side around E_v , which leads to the following formulas:

$$\frac{2m_0}{\hbar^2} \int_0^d (y_1^E)^2 = A_{21}(E) \frac{dA_{11}(E)}{dE} - A_{11}(E) \frac{dA_{21}(E)}{dE}, \quad (\text{B9})$$

$$\frac{2m_0}{\hbar^2} \int_0^d y_1^E y_2^E = A_{11}(E) \frac{dA_{11}(E)}{dE} - A_{12}(E) \frac{dA_{21}(E)}{dE}, \quad (\text{B10})$$

$$\frac{2m_0}{\hbar^2} \int_0^d (y_2^E)^2 = A_{11}(E) \frac{dA_{12}(E)}{dE} - A_{12}(E) \frac{dA_{11}(E)}{dE}, \quad (\text{B11})$$

where E_v was replaced by E . These formulas were necessary for the normalization of the Bloch functions.

Finally, the Wronskian of y_1^E and y_2^E (equal to 1) may be written as

$$(y_1^E)^2 \frac{d}{dz} \left[\frac{y_2^E}{y_1^E} \right] = 1. \quad (\text{B12})$$

Integrating this by parts from 0 to d we obtain

$$A_{11}(E) A_{12}(E) - 2 \int_0^d \frac{dy_1^E}{dz} y_2^E = d, \quad (\text{B13})$$

where, again, we used Eqs. (7) and (8). As we can see, many important quantities can be expressed by the transfer matrix.

*On leave from UNIPRESS, Polish Academy of Sciences, Sokolowska 29, 01-142 Warsaw, Poland.

¹M. Atarelli, in *Semiconductor Superlattices and Heterojunctions*, edited by G. Allan and G. Bastard (Springer-Verlag, Berlin, 1986), p. 12; in *Interfaces, Quantum Wells and Superlattices*, edited by R. Leavens and Roger Taylor (Plenum, New York, 1988).

²V. A. Volkov and T. N. Pinsker, *Surf. Sci.* **81**, 181 (1979); *Zh. Eksp. Teor. Fiz.* **70**, 2268 (1976) [*Sov. Phys.—JETP* **43**, 1183 (1976)]; **72**, 1087 (1977) [**45**, 568 (1977)].

³L. J. Sham and M. Nakayama, *Phys. Rev. B* **20**, 734 (1979).

⁴P. J. Price, in *Proceedings of the International Conference on the Physics of Semiconductors*, Exeter, 1962 (Institute of Physics and the Physical Society, London, 1962), p. 99.

⁵H. Kroemer and Qi-Gao Zhu, *J. Vac. Sci. Technol.* **21**, 551 (1982); Qi-Gao Zhu and H. Kroemer, *Phys. Rev. B* **27**, 3519 (1983).

⁶T. Ando and S. Mori, *Surf. Sci.* **113**, 124 (1982); A. Ishibashi *et al.*, *J. Appl. Phys.* **59**, 4087 (1986).

⁷S. R. White, G. E. Marques, and L. J. Sham, *J. Vac. Sci. Technol.* **21**, 544 (1982).

⁸W. Trzeciakowski, *Phys. Rev. B* **38**, 4322 (1988).

⁹G. Bastard, *Phys. Rev. B* **24**, 5693 (1981).

¹⁰R. A. Morrow and K. R. Brownstein, *Phys. Rev. B* **30**, 678 (1984); R. A. Morrow, **35**, 8074 (1987); **36**, 4836 (1987).

¹¹Y. C. Chang, J. N. Schulman, G. Bastard, Y. Guldner, and M. Voos, *Phys. Rev. B* **31**, 2557 (1985); Y. R. Lin-Liu and L. J. Sham, *ibid.* **32**, 5561 (1985).

¹²There is an interesting numerical study of BC including Γ and

X states in GaAs/Ga_xAl_{1-x}As by H. Akera, S. Wakahara, and T. Ando, *Surf. Sci.* **196**, 694 (1988); see also T. Ando and H. Akera, in *Proceedings of the 19th International Conference on the Physics of Semiconductors*, Warsaw, Poland 1988 (unpublished).

¹³M.-H. Meynadier *et al.*, *Phys. Rev. Lett.* **60** 1338 (1988); E. Finkman, M. D. Sturge, and M. C. Tamargo, *Appl. Phys. Lett.* **49**, 1299 (1986); G. Duggan and H. J. Ralph, in *Quantum Well and Superlattice Physics*, Vol. 792 of *SPIE Proceedings*, edited by H. Dohler and J. N. Schulman (SPIE, 1987), p. 147.

¹⁴E. E. Mendez, E. Calleja, and W. J. Wang, *Phys. Rev. B* **34**, 6026 (1986); E. E. Mendez, W. I. Wang, E. Calleja, and C. E. T. Goncalves da Silva, *Appl. Phys. Lett.* **50**, 1263 (1987); N. R. Couch *et al.*, *Semicond. Sci. Technol.* **2**, 244 (1987).

¹⁵M. Altarelli, in *Applications of High Magnetic Fields in Semiconductor Physics*, edited by G. Landwehr (Springer, Berlin, 1983), p. 174.

¹⁶S. R. White and L. J. Sham, *Phys. Rev. Lett.* **47**, 879 (1981); G. E. Marques and L. J. Sham, *Surf. Sci.* **113**, 131 (1982).

¹⁷V. Heine, *Proc. Phys. Soc. London* **81**, 300 (1963).

¹⁸M. F. H. Schuurmans and G. W. 't Hooft, *Phys. Rev. B* **31**, 8041 (1985).

¹⁹R. Eppenga, M. F. H. Schuurmans, and S. Colak, *Phys. Rev. B* **36**, 1554 (1987).

²⁰R. J. Taylor and M. G. Burt, *Semicond. Sci. Technol.* **2**, 485 (1987).

²¹H. M. James, *Phys. Rev.* **76**, 1602 (1949); **76**, 1611 (1949).

²²W. Kohn, *Phys. Rev.* **115**, 809 (1959).

- ²³E. J. Blount, in *Solid State Physics*, edited by F. Seitz and D. Turnbull (Academic, New York, 1962), Vol. 13, Appendix C.
- ²⁴G. Allen, *Phys. Rev.* **91**, 531 (1953).
- ²⁵In order to have the eigenstates changing smoothly when we go from one band edge to another we have to multiply certain eigenstates by a phase factor $e^{i\phi(E)}$, e.g., across the gap at $k=0$ where the valence-band edge corresponds to $A_{12}(E_v)=0$ and the conduction-band edge to $A_{21}(E_c)=0$ we should multiply the $[a_-, b_-]$ solution by $\exp[i\pi(E-E_v)/(E_c-E_v)]$.
- ²⁶G. L. Bir and G. E. Pikus, *Symmetry and Strain Induced Effects in Semiconductors* (Wiley, New York, 1974).
- ²⁷All generalizations to the 3D case are difficult because in 1D there are only two possible symmetries of the band edges and also band minima can be either at Γ or at X but not at both Γ and X .
- ²⁸As we agreed with M. Altarelli, the two-band BC [Eqs. (78)–(80)] imply the one-band condition [Eq. (2)] but not vice versa. See also Ref. 20.
- ²⁹A. R. Bonnefoi, T. C. McGill, R. D. Burnham, and G. B. Anderson, *Appl. Phys. Lett.* **50**, 344 (1987); A. R. Bonnefoi, T. C. McGill, and R. B. Burnham, *Phys. Rev. B* **37**, 8754 (1988).
- ³⁰H. Neff, K. J. Bachman, and W. D. Laidig, *Superlatt. Microstruct.* **2**, 247 (1986); W. Zhuang *et al.*, *Chin. Phys. Lett.* **3**, 533 (1986); Y. R. Yuan, M.A.A. Pudensi, G. A. Vawter, and J. L. Merz, *J. Appl. Phys.* **58**, 397 (1985).
- ³¹R. People, Y. C. Bean, and D. V. Lang, *J. Vac. Sci. Technol. A* **3**, 846 (1985).
- ³²R. D. Bringans, M. A. Olmstead, R. I. G. Uhrberg, and R. Z. Bachrach, *Phys. Rev. B* **36**, 9569 (1987); F. Herman, *Int. J. Quantum Chem.* **19**, 547 (1985).
- ³³G. A. Sai-Halasz, R. Tsu, and L. Esaki, *Appl. Phys. Lett.* **30**, 651 (1977); G. A. Sai-Halasz, L. Esaki, and W. A. Harrison, *Phys. Rev. B* **18**, 2812 (1978); M. Attarelli, *ibid.* **28**, 842 (1983).
- ³⁴W. Zawadzki, in *Narrow-gap Semiconductors, Physics and Applications*, Vol. 133 of *Lecture Notes in Physics*, edited by W. Zawadzki (Springer-Verlag, New York, 1980), p. 85.